The Lennard-Jones Function: A Quantitative Description of the Spatial Correlation of Electrons As Determined by the Exclusion Principle

Ronald J. Gillespie, David Bayles, James Platts, George L. Heard, and R. F. W. Bader*

Department of Chemistry, McMaster University, Hamilton, Ontario L8S 4M1, Canada

Received: December 29, 1997; In Final Form: March 11, 1998

Lennard-Jones was among the earliest to stress the dominant role played by the exclusion principle in chemistry and was the first to exploit the properties of the same-spin pair density to demonstrate the most probable spatial distribution of a given number of electron pairs. This paper demonstrates that a related distribution function, the conditional probability for same-spin electrons, is so successful in recovering the geometrical models associated with differing numbers of electron pairs, as suggested by the work of Lennard-Jones and subsequently adopted as the basis for the VSEPR model, that we propose that it be called the Lennard-Jones function, or LJF. The maxima in LJF show where the density of the other electrons is most likely to be found, relative to a fixed position of a same-spin reference electron. The digonal, trigonal, tetrahedral, bipyramidal, and octahedral patterns of maxima obtained in such displays demonstrate that these are the most probable arrangements for corresponding numbers of electron pairs. LJF provides a quantitative measure of the extent of exclusion of the density of one electron from that of another of the same spin. There is a remarkable similarity in the patterns of spatial pairing exhibited by LJF and $L(\mathbf{r}) = -\nabla^2\rho(\mathbf{r})$, and the manner in which the two-electron correlation contained in LJF is transmitted to the density and hence to $L(\mathbf{r})$ is accounted for.

Lennard-Jones and the Electron Pair

In an address to the British Association for the Advancement of Science in 1954 Lennard-Jones stated:[1]

"Electrons of like spin tend to avoid each other. This effect is more powerful, much more powerful than that of electrostatic forces. It does more to determine the properties and shapes of molecules than any other single factor. It is the exclusion principle which plays the dominant role in chemistry. Its all-pervading influence does not seem to have been fully realized by chemists, but it is safe to say that ultimately it will be regarded as the most important property to be learned by those concerned with molecular structure."

These remarks followed a number of investigations by Lennard-Jones wherein he demonstrated that the operation of the Pauli exclusion principle keeps electrons of like spin maximally separated, independent of their electrostatic interactions. He and Pople showed, using simple approximations to the orbitals in atoms and some molecules, that the most probable interelectronic angle equaled 180° for two electrons, equaled 120° for three, and assumed the tetrahedral value for four electrons.[2−4]

Within the orbital model, the requirement of the Pauli exclusion principle that the wave function be antisymmetric with respect to the interchange of any pair of electrons is met by limiting the population of a given space orbital to two electrons of opposite spin. This simple consequence of antisymmetry within the orbital model tends to obscure the more fundamental nature of the exclusion principle. The work of Lennard-Jones focused attention on the consequences of the antisymmetry requirement beyond the orbital model. He did this in two ways: by demonstrating, as had others,[5−7] that the corresponding many-electron wave function attains a maximum value for particular relative arrangements of a given number of same-spin electrons[1] and by evaluating the probability distribution function for two same-spin electrons.[2−4]

The first method attempts to give the relative positions of all the electrons simultaneously, which places the results in a nonphysical many-dimensional space. One may, as Lennard-Jones did in this approach, fix the positions of all electrons but one and then search for the position of the remaining electron that maximizes the value of the wave function. One of the authors (R.J.G.) used such descriptions of the most probable relative positions of the electrons in establishing the set of rules underlying the VSEPR model of molecular geometry.[8−10]

The second method makes use of the fact that it unnecessary to know the relative coordinates of all the electrons simultaneously to determine the properties of a molecule. Instead, it is sufficient to know the relative probability of two electrons being in prescribed positions, information given by the two-electron density distribution, also known as the pair density. Its integration over the coordinates of the two electrons, that is, over the space of each electron, yields the total number of electron pairs, just as integration of the one-electron density yields the total number of electrons. By fixing the coordinates of one electron of given spin, the so-called reference electron, one can obtain a map in the real space of the second electron, which can be of either spin, that indicates its most likely position relative to that of the reference electron. Lennard-Jones' arguments are based on the two-electron density for same-spin electrons which he termed the *space-correlation function*. While he had to approximate the orbitals appearing in the space-correlation function in terms of linear combinations of simple Slater atomic-like functions, he was still able to determine the principal angular form of the relative distribution function for a given number of same-spin electrons.

S1089-5639(98)00592-1 CCC: $15.00
Published on Web 04/23/1998

Isolating the Exclusion Effect in Terms of the Fermi Hole

Later investigations of the pair density introduced and focused on the concept of the Fermi hole, that part of the two-electron distribution function that isolates the effect of the exclusion principle on the spatial correlation of same-spin electrons.[11−13] The density of the Fermi hole for a fixed position of a reference electron determines the extent to which the density of another same-spin electron is excluded from its neighborhood. This function integrates to minus one electron, and the Fermi-hole density thus describes how the density of the reference electron is spread out in space, thereby excluding an equivalent amount of same-spin density. With this interpretation, it is clear that if the density of the Fermi hole is spatially localized, then so is the reference electron.[13]

The Fermi hole correlates only the motions of same-spin electrons. In the field of a central nucleus it is the existence of the potential wells created by the presence of the ligands that leads to the formation of $\alpha\beta$ electron pairs by the trapping of the localized Fermi holes in the potential wells of the ligands. Since only electrons of like spin are excluded from a localized Fermi hole, then, in a closed-shell molecule, the spatial localization of an α spin electron implies the equivalent localization of another of β spin and the result is the formation of a localized pair. From this point of view, the minimum energy molecular geometry should be obtained when the spatial arrangement of the potential wells determined by the relative orientation of the ligands is coincident with the most probable arrangement of the localized Fermi holes.

A review[14] of how the properties of the Fermi-hole density can be used to determine the extent of the spatial pairing of electrons and of how this localization is reflected in the topologies of the laplacian of the electron density[15] and of the electron localization function of Becke and Edgecombe[16] has appeared recently. The paper relates the properties of these two functions to a quantity termed the conditional probability, the probability of finding an electron of given spin at position $\mathbf{r}_2$, conditional upon the same-spin reference electron being at $\mathbf{r}_1$. The form of this function was discussed and illustrated in terms of its two contributing densities, the α spin density at position $\mathbf{r}_2$, $\rho^\alpha(\mathbf{r}_2)$, and the density of the Fermi hole, $h^\alpha(\mathbf{r}_1,\mathbf{r}_2)$, whose definition in terms of the Hartree−Fock orbitals is given in refs 13 and 14. The latter density is a negative quantity corresponding to the decrease in the value of the same-spin density at $\mathbf{r}_2$ because of the spreading out of the density of the reference electron with coordinate $\mathbf{r}_1$.

In this paper we show that the spatial distribution of the electron pairs suggested by Lennard-Jones' studies of the space-correlation function[4] can be recovered in terms of the properties of the conditional probability. Indeed so successful is the conditional probability in recovering the geometrical models associated with differing numbers of electron pairs as suggested by the work of Lennard-Jones and subsequently adopted as the basis of the VSEPR model[8,9] that we suggest the conditional probability for same-spin electrons be called the Lennard-Jones function, or LJF.

The Lennard-Jones Function

The conditional probability can be defined at any level of theory that includes antisymmetrization of the wave function. The effect of antisymmetrization is so pronounced and the resulting correlation of the motions of same-spin electrons so strong that even the simplest of these theories, the Hartree−Fock single-determinant model, provides an excellent description of the density of the Fermi hole and the associated exclusion effects.[17] In this orbital product model, each electron moves in the average field of the remaining electrons, and hence there is no correlation of the motions of electrons of different spin. However, the orbital exchange introduced by the antisymmetrization of the product function results in the correlation of same-spin electrons, often called exchange correlation. Introducing the so-called Coulomb correlation between the electrons by proceeding beyond the Hartree−Fock approximation has only minor effects on the density of the Fermi hole. Thus the Hartree−Fock wave function, since it correlates only same-spin electrons, is ideal for illustrating the effects of the exclusion principle.

Since the Hartree−Fock pair density for electrons of different spin is uncorrelated, the $\alpha\beta$ pair density is given simply by the product of the α- and β-spin densities multiplied by one-half so as not to count the same pair twice,

$$\rho^{\alpha\beta}(\mathbf{r}_1,\mathbf{r}_2) = (1/2)\rho^\alpha(\mathbf{r}_1)\rho^\beta(\mathbf{r}_2) \qquad (1)$$

with a corresponding expression for the $\beta\alpha$ pair density. Because of the presence of the exchange correlation for same-spin electrons however, the same-spin α density at $\mathbf{r}_2$, $\rho^\alpha(\mathbf{r}_2)$, is reduced in value by the density of the Fermi hole, and the $\alpha\alpha$ two-electron density, the space-correlation function of Lennard-Jones,[4] is given by

$$\rho^{\alpha\alpha}(\mathbf{r}_1,\mathbf{r}_2) = (1/2)\rho^\alpha(\mathbf{r}_1)\{\rho^\alpha(\mathbf{r}_2) + h^\alpha(\mathbf{r}_1,\mathbf{r}_2)\} \qquad (2)$$

The term in curly brackets is *the conditional probability*, $\delta^\alpha(\mathbf{r}_2,\mathbf{r}_1)$, or LJF. It is the difference between $\rho^\alpha(\mathbf{r}_2)$, the spin density at $\mathbf{r}_2$, and the magnitude of the Fermi-hole density at $\mathbf{r}_2$ for a given position $\mathbf{r}_1$ of the reference electron. Thus the space-correlation function is given by $(1/2)\rho^\alpha(\mathbf{r}_1)\ \delta^\alpha(\mathbf{r}_2,\mathbf{r}_1)$.

The conditional probability $\delta^\alpha(\mathbf{r}_2,\mathbf{r}_1)$ is, therefore, *a measure of the amount of same-spin density not excluded from the position* $\mathbf{r}_2$ *by the spreading out of the density of the reference electron at* $\mathbf{r}_1$. Clearly, the maxima in a plot of $\delta^\alpha(\mathbf{r}_2,\mathbf{r}_1)$ for a fixed position of the reference electron will show where the density of the remaining same-spin electrons is most likely to be found.

The Fermi-hole density equals the spin density when $\mathbf{r}_1 = \mathbf{r}_2$, thereby totally excluding all other same-spin density from the position of the reference electron. Consequently when $\mathbf{r}_1 = \mathbf{r}_2$, $\delta^\alpha(\mathbf{r}_1,\mathbf{r}_1) = 0$. The integral of $\delta^\alpha(\mathbf{r}_2,\mathbf{r}_1)$ over the space of the second electron equals $N^\alpha - 1$. That is, $\delta^\alpha(\mathbf{r}_2,\mathbf{r}_1)$ describes the spatial disposition of the remaining same-spin electrons for a given position of the reference electron. A program has been written to locate and characterize the critical points in LJF. In this situation, $\delta^\alpha(\mathbf{r}_2,\mathbf{r}_1)$ is expressed as a function of $\mathbf{r}_2$ for a fixed position of the reference electron $\mathbf{r}_1$ and a critical point corresponds to the vanishing of the gradient of $\delta^\alpha(\mathbf{r}_2,\mathbf{r}_1)$ with respect to the coordinate $\mathbf{r}_2$. Of primary interest are the number and location of the local maxima in LJF, critical points in $\delta^\alpha(\mathbf{r}_2,\mathbf{r}_1)$ where all three curvatures are negative. LJF attains its maximum value at a point where the density of the Fermi hole vanishes, the value of LJF then equaling the spin density $\rho^\alpha(\mathbf{r}_2)$, eq 2. Thus the ratio $\delta^\alpha(\mathbf{r}_2,\mathbf{r}_1)/\rho^\alpha(\mathbf{r}_2)$ is a measure of the degree of exclusion of the density of the reference electron with coordinate $\mathbf{r}_1$ from the point $\mathbf{r}_2$, and when multiplied by 100%, it yields a percentage measure of the effect of the Pauli exclusion principle. This ratio, denoted by $X(\mathbf{r}_2,\mathbf{r}_1)$, is the percent *exclusion* of the density of the reference electron from the point $\mathbf{r}_2$.

From eq 2, the decrease in the same-spin pair density for a given $\mathbf{r}_1$ and $\mathbf{r}_2$ is determined by the product $\rho^\alpha(\mathbf{r}_1)h^\alpha(\mathbf{r}_1,\mathbf{r}_2)$,

which equals the Hartree−Fock exchange density. The total number of same-spin electrons excluded from a region of space Ω, a quantity denoted by $F^{\alpha\alpha}(\Omega,\Omega)$, is obtained by the corresponding integration of this product over the coordinates of both electrons.[13] The limiting value of $F^{\alpha\alpha}(\Omega,\Omega)$ is $-N^{\alpha}(\Omega)$, the spin population of region Ω. Thus the ratio $|F^{\alpha\alpha}(\Omega,\Omega)|/N^{\alpha}(\Omega)$ is a measure of the degree of localization of the α electrons in Ω, because when this ratio equals unity, it implies that the Fermi density for the electrons in Ω is totally contained in Ω, thereby excluding all other same-spin electrons from Ω. In this unattainable but approachable limit, there is no exchange of the electrons inside Ω with those outside of Ω, and they form two separately localized sets. When multiplied by 100%, this ratio yields $l(\Omega)$, the percent *localization* of the electrons in Ω.[13]

The populations and Fermi correlations reported here are for atoms, regions of space bounded by surfaces of local zero flux in $\nabla\rho$.[18] Atoms and their properties are defined by the quantum action principle and consequently are proper open systems.[19] All properties of such open systems are additive to yield the molecular values. The properties predicted in this manner recover the experimentally determined contributions to the volume, energy, polarizability, and magnetic susceptibility in those cases where the results give evidence of atomic or group contributions that are transferable,[20] in addition to being additive. The wave functions were calculated using GAUSSIAN 94 with the 6-311++G(2d,2p) basis set.[21] All of the critical points in LJF discussed in the paper have been located and characterized.

The electrons in the core orbitals are omitted from the calculations of LJF. These electrons are strongly localized[13,14] and the full spin density of the core appears in the displays of LJF for any position of the reference electron removed from the core region. Since the outer density of a core extends into the valence region, the associated contours obscure the behavior of the valence electrons of the central atom. This is illustrated and discussed below in the case of PH_3.

In what follows we demonstrate that the conditional probability $\delta^{\alpha}(\mathbf{r}_2,\mathbf{r}_1)$ or Lennard-Jones function establishes the most favored patterns of electron localization for two, three, four, five, and six pairs of electrons, patterns that are in full accord with the patterns of electron domains assumed in the VSEPR model.[9] It is also found that the localization patterns defined by LJF can be mapped to a remarkable degree onto the maxima in the negative of the Laplacian of the electron density, the quantity $L(\mathbf{r}) = -\nabla^2\rho(\mathbf{r})$, found in the valence shell charge concentration VSCC of an atom. The maxima in $L(\mathbf{r})$ determine the positions within a molecule where the electronic charge is maximally concentrated. The number, angular distribution, and relative size of these charge concentrations CCs have been shown to recover the properties of the electron domains of the VSEPR model.[15]

LJF for Two and Three Electron Pairs. The molecules BeH_2 and BH_3 contain respectively two and three pairs of valence electrons, the valence density being found largely within the basins of the hydrogen atoms. The net charges on the hydrogen atoms, as determined by the integration of the density over the atomic basins,[20] are −0.87e and −0.70e, respectively.

In Figure 1a the reference electron, hereafter referred to as e*, is situated at the position of one of the protons in BeH_2, and the LJF plot shows that the density of the second same-spin electron is strongly localized within the basin of the second hydrogen atom. The small amount of spin density appearing in the basin of the beryllium atom is from the valence orbitals that extend into its core region. Alternatively, one can interpret

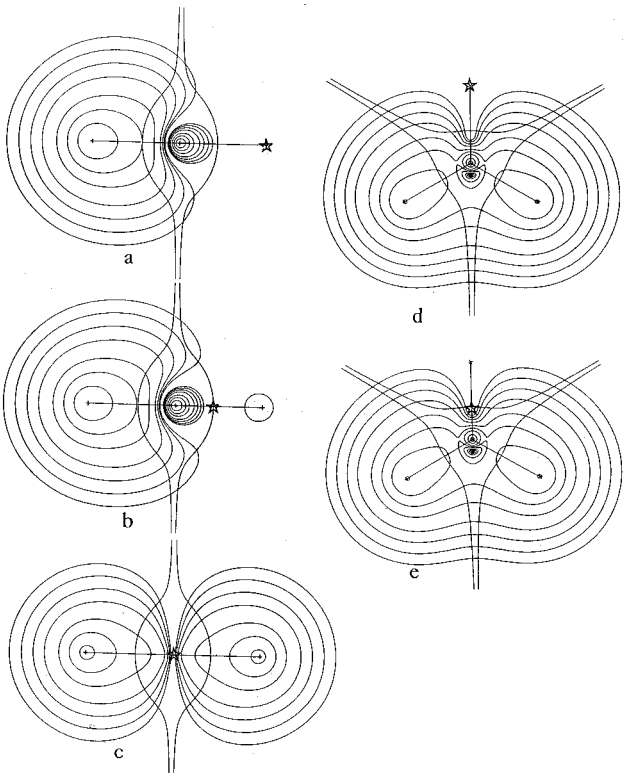

Figure 1. Contour maps of the Lennard-Jones function LJF for BeH_2 and BH_3. The boundaries of the atomic basins and the bond paths are shown on each map. The position of the reference electron is denoted by a star and is referred to as e*. LJF equals zero at the position of e*. The contours increase in value from this point and inward from the exterior of the molecule, starting at 0.001 au and then in steps of 2×10^n, 4×10^n, and 8×10^n with n beginning at −3 and increasing in steps of unity. (a) e* is at the position of a proton in BeH_2, and LJF is essentially zero over the associated basin. (b) e* is moved to the Be−H bond critical point, and the second same-spin electron remains almost totally excluded from the starred basin. (c) e* is at the Be nucleus. (d) e* is at a proton in BH_3. (e) e* is at a B−H bond critical point.

the same diagram as showing that nearly all the density of the second same-spin electron is excluded from the basin of the atom containing e*. Correspondingly, the percent exclusion $X(\mathbf{r}_2,\mathbf{r}_1)$ equals 99% at the maximum in the basin of the second hydrogen. When $X(\mathbf{r}_2,\mathbf{r}_1) = 100\%$, the pair density reduces to one α,β pair at $\mathbf{r}_1$ and another at $\mathbf{r}_2$. While LJF always equals zero at the position of e*, the essentially complete removal of all other same-spin density from the basin containing e* indicates that the Fermi-hole density $h^{\alpha}(\mathbf{r}_1,\mathbf{r}_2)$ equals $-\rho^{\alpha}(\mathbf{r}_2)$ over the entire basin and the Fermi hole is localized.

This localization is little changed for motion of e* within the basin of the first proton. Thus as illustrated in Figure 1b, even when e* is placed at the Be−H bond critical point, that is, on the boundary separating the two atoms, only a small amount of same-spin density appears in the basin of the reference atom and $X(\mathbf{r}_2,\mathbf{r}_1)$ at the maximum in LJF remains equal to 99%. Since the same behavior is obtained for the electrons of either spin, the valence pair density for this molecule is well represented by two pairs of electrons, each pair localized within the basin of a hydrogen atom. When the reference electron is placed at the position of the beryllium nucleus, Figure 1c, the density of the second same-spin electron is equally delocalized over the basins of both hydrogen atoms. In this case, both α electrons contribute equally to both hydrogen atom basins, a situation corresponding to the maximum delocalization of the valence electrons, and $X(\mathbf{r}_2,\mathbf{r}_1)$ decreases to 56% at both maxima. However, since the valence density lies primarily

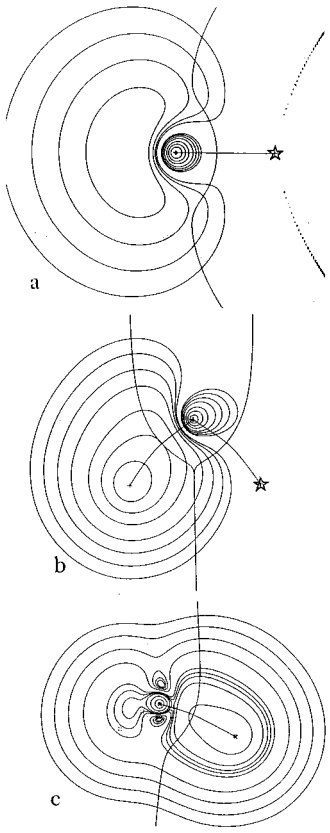

Figure 2. Contour maps of LJF. (a) e* is at the proton in BeH^- (to be compared with 1a). (b) e* is at a proton in 90° bent BeH_2. (c) e* is on an out-of-plane proton in pyramidal BH_3. Two extra contours of value 0.025 and 0.30 au are present to indicate the small maxima formed along the 3-fold axis above and below the B nucleus.

within the basins of the hydrogen atoms, this pattern of delocalization contributes little to the total pair density.

Similar results are obtained for the BH_3 molecule. Figures 1d and 1e show the localization of the density of the two same-spin electrons in the basins of two of the hydrogen atoms when e* is placed within the basin of the third hydrogen atom or on its boundary. As in BeH_2, the same-spin density is delocalized over the basins of all three hydrogen atoms when e* is placed at the position of the boron nucleus, the value of $X(\mathbf{r}_2,\mathbf{r}_1)$ at the maxima decreasing from 99% to 74% when e* is moved from a proton to the boron nucleus. These results are in accord with previous studies of the localization of the Fermi correlation in these molecules which show that they are well described by a localized pair on the core of the metal atom and a valence pair localized on each of the hydrogens.[13] The electrons of either spin are 90% localized within the basins of the hydrogen atoms in BeH_2 and 77% in BH_3, as measured by $l(\Omega)$.

The maps in Figure 1 show a coincidence of the localized Fermi holes and the positions of the potential wells within the basins of the hydrogen atoms, as anticipated for equilibrium geometries. They do not, however, separate the effect of correlation from the electrostatic effect associated with the potential wells. The operation of the two effects separately from one another can be illustrated in two ways.

Figure 2a shows LJF for BeH^- with e* at the proton. The map is essentially the same as Figure 1a for BeH_2. It demonstrates that the second same-spin electron is excluded from the basin containing e* and is maximally separated from it by the Fermi correlation, even in the absence of a second proton. The LJF density is, however, more diffuse since its maximum, for which $X(\mathbf{r}_2,\mathbf{r}_1) = 92\%$, is created in the absence of a proton. The electrons within the basin of the hydrogen atom are only slightly less localized than in BeH_2, with $l(H) = 93\%$.

Figure 2b shows that upon bending the BeH_2 molecule with e* positioned at a proton, the density of the second electron lags behind the motion of the proton and it spreads into the basin of the beryllium atom, as well as into the basin of the hydrogen containing e*. While the value of $X(\mathbf{r}_2,\mathbf{r}_1)$ remains essentially unchanged at the maxima in LJF, there is a pronounced decrease in the degree of localization of the electrons within the basins of each hydrogen atom, the values decreasing to 86% for bent (90°) BeH_2 and to 74% for pyramidal (109.5°) BH_3, Figure 2c. Thus when the Fermi hole is displaced by a change in geometry, it becomes less localized. The minimum energy geometries in these two molecules are obtained when the Fermi holes are maximally localized within the ligand potential wells.

The spatial displays of electron localization depicted by LJF in these two molecules are of the same form and possess the same number and location of maxima as exhibited in maps of $L(\mathbf{r})$. In fact, placing e* at the position of a charge concentration (CC) in the Laplacian yields, in general, the most localized associated LJF description, and this procedure is used in many of the plots that follow.

LJF for Four Electron Pairs. The maps for PH_3, Figure 3, illustrate a number of the general features of LJF. Placing e* at the position of the nonbonding CC in $L(\mathbf{r})$, Figure 3a, leads to the exclusion of same-spin density from the region associated with the lone pair within the basin of the phosphorus atom and to its accumulation within each of the hydrogen atomic basins, with maxima located at the protons, as they are in $L(\mathbf{r})$. Similarly, placing e* at the position of a proton, that is, at a bonded maximum in $L(\mathbf{r})$, Figure 3b,c, leads to the exclusion of all same-spin density from its vicinity and to its localization at the position of the lone pair within the phosphorus atomic basin and within the basins of the remaining two hydrogen atoms. Clearly, this tetrahedral-like pattern of electron localization which includes the lone pair region and displayed in Figure 6, is not driven simply by the positioning of the three potential wells of the protons.

These maps are insensitive to where e* is placed between the nuclei along a P−H axis or where on the nonbonded side of the phosphorus atom on the 3-fold symmetry axis, the values of $X(\mathbf{r}_2,\mathbf{r}_1)$ varying from 97 to 100%. Moving e* to a position on the 3-fold axis on the bonded side of the phosphorus atom, however, causes a significant decrease in the localization of LJF, with spin density appearing in all four tetrahedral regions, Figure 3d, and the value of $X(\mathbf{r}_2,\mathbf{r}_1)$ decreasing to 72% at the maxima in each of the hydrogen basins.

Figures 3e and 3f show LJF for PH_3 obtained with the core orbitals retained in the calculation. In these maps e* is placed at the position of a proton, and each map is to be compared with its corresponding map with the core excluded, maps 3b and 3c. The purely valence contours, those up to 0.02 au, are superimposable for each pair of maps. The maximum at the position of a proton is unchanged, but the maximum associated with the nonbonding electron in the VSCC of phosphorus is now contiguous with the spin density of the core and is present as a shoulder in the total display. Map 3f is in fact superimposable on a map of the α spin density, contour for contour, in the nonbonding region along the 3-fold axis, as well as over the whole of the core. This implies that the density of e* is totally excluded from the nonbonded and core regions, and the

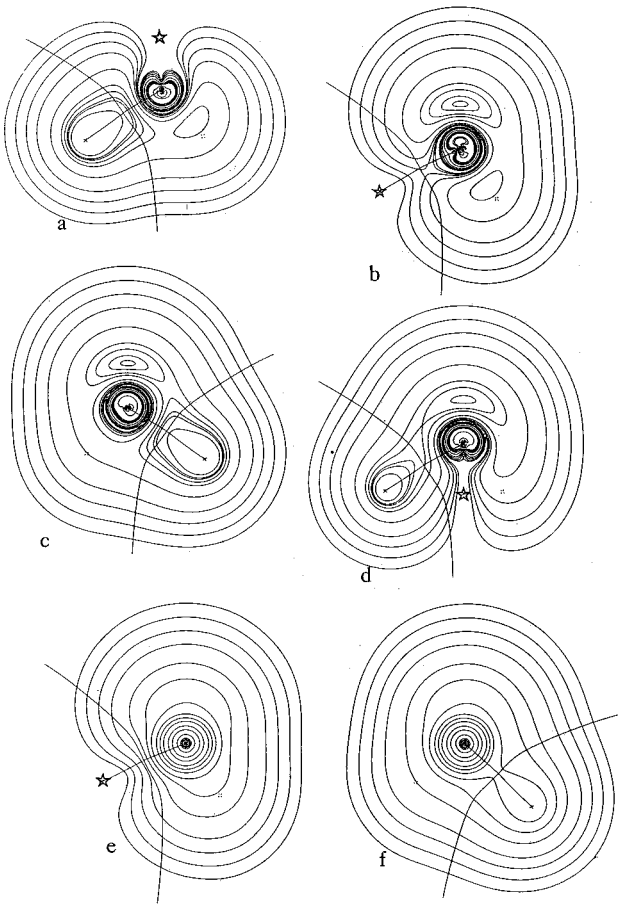

Figure 3. Contour maps of LJF for PH_3 with the added contours 0.05, 0.06, and 0.065 au. (a) e* is at the position of the nonbonding CC in $L(\mathbf{r})$, and maxima in the same-spin density appear on each of the protons. The projected positions of out-of plane nuclei are indicated by an open cross. The apparent maximum lying between the two out-of-plane protons in (a) and (b) is only two-dimensional. It is a $(3,-1)$ critical point linking the two associated out-of-plane maxima. (b) e* is at a proton, and maxima appear at the position of the nonbonding CC on phosphorus (inner contour value of 0.065 au) and at the positions of the two out-of-plane protons, as indicated by the presence of the $(3,-1)$ critical point. (c) e* is on an out-of-plane proton, and maxima are found in the nonbonding region and on the two remaining protons. (d) e* is on the 3-fold axis opposite the nonbonded maximum. Same-spin density appears in all four tetrahedral positions, showing that the density of the reference electron is delocalized over all four regions. The maxima are consequently decreased in extent and value. Maps (e) and (f) include the core density, and e* is on a proton, out-of-plane in (f). Each map is superimposable with its counterpart with the core excluded, (b) and (c) respectively, up to the outer contour of the nonbonding maximum.

sum of the LJ functions for both the α and β electrons will equal the total density of the molecule in the nonbonded region and the core. Clearly, the accumulation of nonbonding spin density would be revealed in a plot of the Laplacian of LJF, since it would be identical to the Laplacian of the density, $L(\mathbf{r})$.

Placing e* at the position of a proton in the H_2S molecule leads to the localization of the same-spin density in the two lone pair regions and within the basin of the second hydrogen atom, Figure 4a,b. Placing e* at the position of a nonbonding CC in $L(\mathbf{r})$ localizes the same-spin density in the basin of each hydrogen and in the second lone pair region, Figure 4c,d, respectively. The values of $X(\mathbf{r}_2,\mathbf{r}_1)$ at the corresponding maxima in LJF are all in excess of 99%, and the patterns of localization are again insensitive to the precise location of e* along the respective bonded or nonbonded axes.

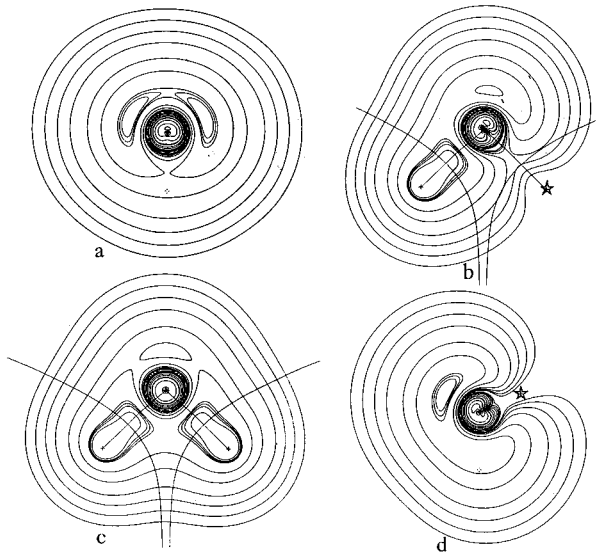

Figure 4. Contour maps of LJF for H_2S with added contours 0.085, 0.090, and 0.10 au. (a) e* is on an out-of-plane proton, showing the two nonbonding maxima with inner contour equal to 0.09 au. (b) e* is on a proton in plane with the nuclei with inner contour on bonding maximum equal to 0.1 au. Out-of-plane nonbonding maxima are also present, as indicated by the intervening pseudomaximum of a $(3,-1)$ critical point. (c) e* is on an out-of-plane nonbonding CC of $L(\mathbf{r})$. (d) e* is on nonbonding CC, showing exclusion of same-spin density from one such region and its accumulation in the other.

The extent of localization of the same-spin density is decreased when PH_3 is made planar or when H_2S is made linear, causing the percent localizations of the spin density within the basins of the hydrogen atoms to decrease from 65 to 61% in PH_3 and from 48 to 30% in H_2S and the values of $X(\mathbf{r}_2,\mathbf{r}_1)$ at the maxima in the hydrogen basins to decrease to 93 and 83%, respectively. These effects are evident in the maps shown in Figure 5. In planar PH_3, with e* at the position of a proton, the nonbonded same-spin density is split into two less localized regions, one on each side of the symmetry plane, and its maximum value > 0.065 attained in the equilibrium geometry is reduced to a value < 0.060 au. In linear H_2S the localization of same-spin density in the bonding region is greatly reduced, and the region becomes contiguous with a torus of nonbonding same-spin density within the basin for the sulfur atom that is less pronounced and less localized than the two corresponding separately localized domains in the bent molecule. The most stable geometries of these two molecules with four valence electron pairs maximize the coincidence of the potential wells of the two protons in H_2S and of the three protons in PH_3 with the tetrahedral pattern of localization of same-spin density exhibited by LJF. Making the geometries planar or linear destroys the tetrahedral pattern of maximum mutual exclusion of the same spin-density and reduces its degree of localization into separate spatial regions.

The LJ function exhibits similar tetrahedral patterns of same-spin localization in the equilibrium geometries of CH_4, NH_3, and H_2O, the only difference being that in these cases where the central atom is more electronegative than its third-row counterpart the bonding spin density associated with a given proton exhibits a maximum at a position along the bond path within the basin of the A atom, as well as at the position of the proton. This same behavior is exhibited by $L(\mathbf{r})$ where both bonding and nonbonding CCs occur within the VSCC of the A atom, in addition to the maxima in $L(\mathbf{r})$ found at the positions of the protons. The values of $X(\mathbf{r}_1,\mathbf{r}_2)$ at the maxima in NH_3 and H_2O are in excess of 99%, and as with PH_3 and H_2S, these

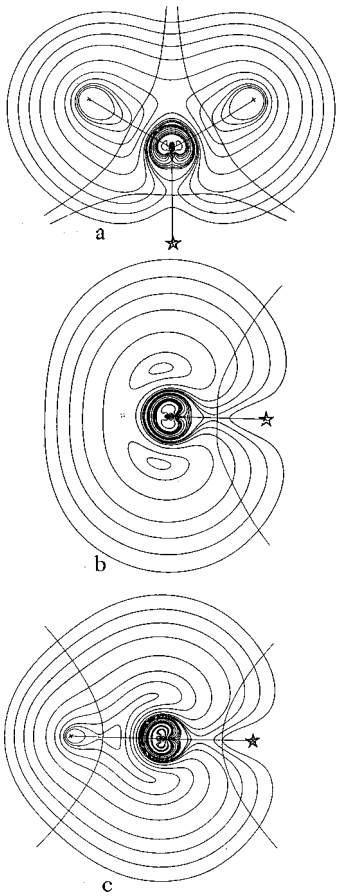

Figure 5. Contour maps of LJF for planar PH_3 and linear H_2S with the same added contours as in Figures 3 and 4, respectively. (a) e* is on a proton in plane with P and H nuclei. (b) e* is on a proton, showing bifurcation of nonbonding same-spin density on P. (c) e* is on a proton in linear H_2S.

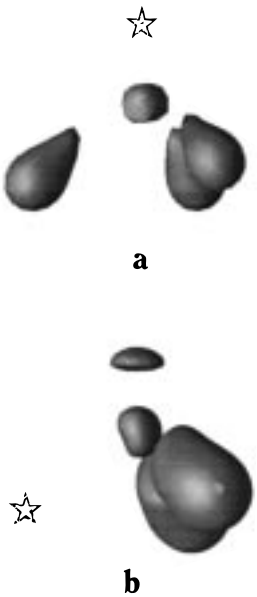

Figure 6. Envelope maps of LJF for PH_3. In (a), e* is at the position of the nonbonding maximum, and the same-spin density is localized on the three protons, envelope value = 0.15 au. In (b) e* is at the position of a proton, and same-spin density is localized on the remaining two protons and in the nonbonding region, envelope value = 0.06 au. Same-spin density is localized within the phosphorus core in both cases.

values and l(H), the localization of the electrons on the hydrogen atoms, decrease when they assume planar and linear geometries,

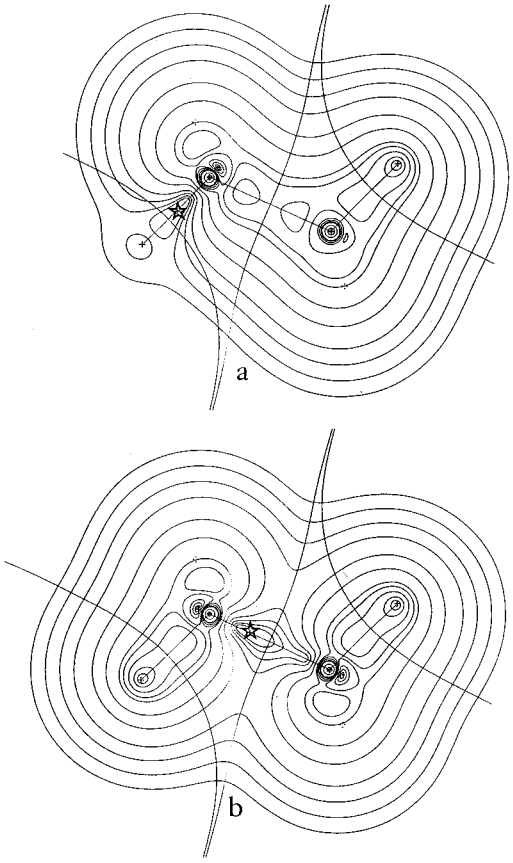

Figure 7. Contour maps of LJF for ethane with added contours 0.10, 0.13, and 0.17 au. (a) e* is on a C−H bonding CC in VSCC of a carbon, showing two C−C bonding same-spin maxima and one of the C−H bonding maxima. (b) e* is on a bonding CC directed at another carbon, which results in the loss of both C−C same-spin maxima.

respectively. As well as the number and relative location of the maxima exhibited by LJF and $L(\mathbf{r})$ being the same, the distances of the maxima from the A nucleus are very similar in both distributions. A maximum in LJF occurs approximately 0.1−0.2 au closer to the A nucleus than the corresponding CC in $L(\mathbf{r})$,[14] the small differences being most likely due to the omission of the core density from the LJF calculations. The angular distribution of the CCs of $L(\mathbf{r})$ in the VSCC of A and the corresponding maxima in LJF are the same to the accuracy of the LJF plots. In H_2O and H_2S these angles subtended at the A nucleus are 128° and 121°, respectively.

The Lennard-Jones function emulates $L(\mathbf{r})$ in the ethane molecule, exhibiting a total of four bonding maxima in the VSCC of each carbon atom for placement of e* at the position of a C−H or C−C bonding CC in $L(\mathbf{r})$, Figure 7a,b. Thus, like $L(\mathbf{r})$, the electron pair associated with the C−C bond is represented by two maxima, one in the VSCC of each carbon. The LJ function enables one to demonstrate that these two maxima represent a single pair of electrons. Locating e* at the position of one such bonding CC results in the removal of both C−C same-spin maxima, with only the six C−H maxima remaining. The value of $X(\mathbf{r}_2,\mathbf{r}_1)$ is in excess of 99% at all of these maxima.

The topology of ELF was first studied by Silvi and Savin.[22] While the pattern of localization determined by ELF exhibits a general homeomorphism with that of $L(\mathbf{r})$, the maxima in ELF generally occur at considerably greater distances from the A nucleus than are found in $L(\mathbf{r})$ and in LJF.[14] The respective values of the radii of the nonbonded maxima in PH_3 and H_2S,

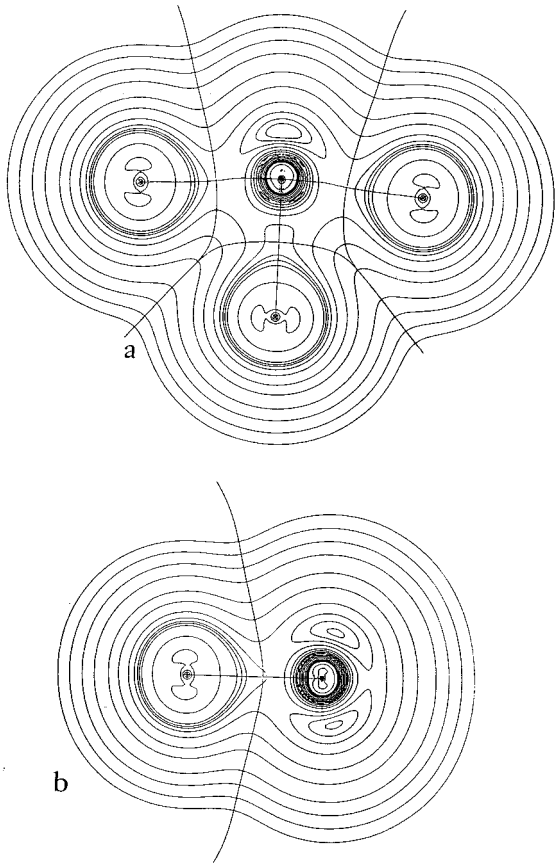

Figure 8. Contour maps of LJF for ClF_5 in (a) and ClF_3 in (b) with added contours 0.12, 0.15, and 0.17 au. e* is on an out-of-plane Cl−F bond critical point in both (a) and (b), equatorial in (a) and axial in (b). The 0.2 au contour encompasses the bond critical point (the intersection of the bond path and interatomic surface) for the axial fluorine in (a).

for example, are 2.3 and 1.9 au in ELF but 1.4 and 1.3, and 1.3 and 1.2 in $L(\mathbf{r})$ and LJF, respectively. In hydrides such as CH_4, NH_3, H_2O, and HCl, the bonded maxima in ELF occur only at the positions of the protons. While such maxima are also found in $L(\mathbf{r})$ and LJF, both these functions exhibit bonded and nonbonded maxima within the VSCC of the A atom.

LJF for Five and Six Electron Pairs. The ClF_3 and ClF_5 molecules possess five and six valence electron pairs, respectively. The displays of LJF in Figure 8 show the two regions of localization of nonbonding same-spin density on the Cl atom in ClF_3 and the single such region in ClF_5 that are obtained when e* is placed at a Cl−F bond critical point. The associated maxima, with $X(\mathbf{r}_2,\mathbf{r}_1)$ values of 97%, occur at approximately the same distance from the Cl nucleus, 1.1 au, as they do in $L(\mathbf{r})$. Unlike $L(\mathbf{r})$, LJF does not exhibit bonding maxima in the VSCC of the Cl atom, but instead localizes the same-spin density within the basin of each F atom. Like $L(\mathbf{r})$, however, the localization that is present is more pronounced for the unique F atom in both molecules, as evidenced by the 0.2 au contour in the region of the bond critical points in the map for ClF_5. LJF also exhibits the same patterns of nonbonding charge localizations within the basins of the F atoms as does $L(\mathbf{r})$.

LJF for Transition Metal Molecules. The topologies of both $L(\mathbf{r})$ and ELF demonstrate that the pattern of electron localization found in transition metal molecules differs from that found in main group elements in two principal ways.[14,23] The first is that in the transition metal molecules the maxima in $L(\mathbf{r})$ and ELF resulting from the interaction with the ligands

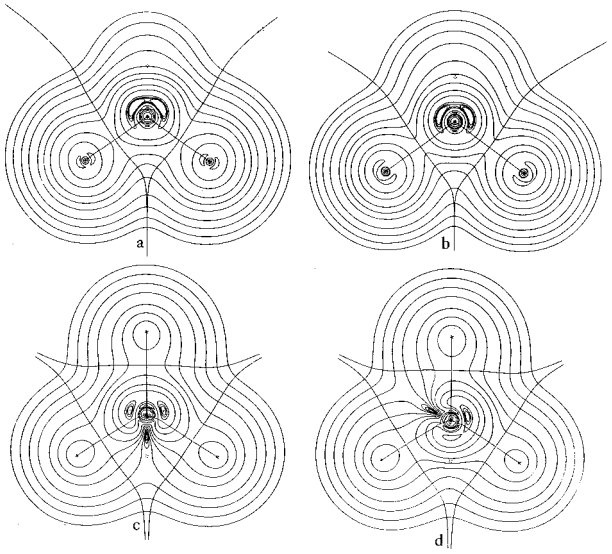

Figure 9. Contour maps of LJF for CrO_2F_2 and VH_5 with added contours 0.90, 0.95, and 1.00 au. (a) e* is on a CC of $L(\mathbf{r})$ opposed to a fluorine, showing the same-spin maxima opposed to the oxygens. (b) e* is on a CC of $L(\mathbf{r})$ opposed to an oxygen, showing the two same-spin maxima opposed to the fluorines. (c) e* is on a CC of $L(\mathbf{r})$ opposed to apical proton, showing same-spin maxima opposed to basal protons. (d) e* is on a CC of $L(\mathbf{r})$ opposed to a basal proton, showing the maxima in same-spin density opposed to the apical and a basal protons.

occur in the outer shell of the core of the metal atom, rather than in its valence shell, the shell structure being defined by either $L(\mathbf{r})$ or ELF.[24] The outer core orbitals, $3s^23p^6$, are included in the calculations of LJF for the transition metal molecules. The second is that these maxima are in general found to be opposed to the ligands rather than adjacent to them in the manner of a bonding CC. In the case of $L(\mathbf{r})$ they are called ligand opposed charge concentrations.[23]

In CrO_2F_2, for example, both $L(\mathbf{r})$ and ELF exhibit four maxima in the region of the outer shell of the Cr atom in an approximate tetrahedral arrangement, and the negatively charged ligands are found not at the vertices of the tetrahedron but in the four faces where the electronic charge is maximally depleted. The maxima opposed to the oxygen atoms are larger than those opposed to the fluorine atoms, thereby causing the F−Cr−F angle to be greater than the O−Cr−O angle, contrary to what would be anticipated if the maxima behaved as bonding maxima. The VH_5 molecule has a square pyramidal rather than the trigonal bipyramidal structure anticipated on the basis of the VSEPR model. The ligands instead occupy positions in each of the faces of the square pyramidal structure defined by the five maxima in either $L(\mathbf{r})$ or ELF, thereby enabling the negatively charged ligands to avoid the charge concentrations as in CrO_2F_2.

The Lennard-Jones function exhibits the same number and arrangement of maxima for both molecules. In Figure 9a, e* is placed at a CC in $L(\mathbf{r})$ opposed to a F in CrO_2F_2, and the map shows a same-spin maximum opposed to each of the oxygen atoms. In Figure 9b, e* is placed at a CC opposed to an oxygen, and the map shows the maximum opposed to each of the fluorine atoms. In each case the third ligand opposed maximum is present in the plane containing e*. The maxima exhibit the same characteristics as those found in $L(\mathbf{r})$: the maxima opposed to the oxygens are larger than those opposing the fluorines; the angle subtended at Cr by the maxima opposed to the fluorines is larger than that formed by those opposed to the oxygens, 120° compared to 100° for both fields; both sets

of maxima are the same distance from the Cr nucleus, 0.60 au for LJF and 0.67 au for $L(\mathbf{r})$. LJF for the VH_5 molecule also exhibits the same form as that found for $L(\mathbf{r})$ and ELF, Figure 9c,d, with the five same-spin maxima defined by LJF forming a square-based pyramid with its vertices opposed to the ligands. The degree of exclusion approaches 100% at the maxima in both molecules.

Discussion

For a given position of e*, the maxima portrayed in the Lennard-Jones function denote the most probable positions of the density of the remaining same-spin electrons, as determined by the Pauli exclusion principle. The patterns of electron localization denoted by these maxima yield the most probable arrangements of two, three, four, five, and six electron pairs anticipated in the VSEPR model of molecular geometry. Mayer[25] has recently argued that the "driving force" behind the VSEPR rules is a consequence of the orthogonality constraints acting on a set of simple hybrid orbitals centered on the central atom. These constraints, however, have meaning only within the orbital model and are themselves but a consequence of the exclusion principle applied to this model.

The localization determined by LJF appears most pronounced for those hydrides in which the hydrogens bear negative charges, and one has spatial localization of the total density as well as of the pair density. In these molecules there is a one-to-one correspondence between the number of maxima in LJF and the assumed number of localized electron pairs, a pattern that is maximized when it coincides with the positions of the potential wells of the ligands that minimize the energy. In the more covalent hydrides, LJF exhibits two maxima for each anticipated bonding electron of given spin, one on the proton and another within the basin of the central atom. A similarly related pair of same-spin maxima is also found for the C−C bonded pair in ethane.

The maxima in the same-spin density of LJF faithfully recover the number and properties of the nonbonding CCs of $L(\mathbf{r})$ found within the VSCC of the central atom in all the molecules studied. The maxima in LJF also recover the pattern and properties of the CCs of $L(\mathbf{r})$ present in the outer shell of the core of the metal atom in a transition metal molecule.

The pairing of electrons is a consequence of the spatial localization of an electron of given spin, as determined by a corresponding localization of its Fermi hole.[13] The maxima in the Lennard-Jones function indicate the number and relative positions of the spatial regions where the same-spin density is localized, as a consequence of the localization of the Fermi-hole density of e*. The most probable of these localization patterns for a given number of same-spin electrons agrees with the empirically determined pattern of the bonding and nonbonding CCs found in the Laplacian of the electron density or by the maxima in ELF.[16] The latter function is determined by a quantity Δ, the difference between the many- and one-electron kinetic energy densities.[26] A vanishing Δ implies a vanishing of the same-spin conditional pair density and the factors causing Δ to vanish are the same as those required for the localization of the density of the Fermi hole.[14,26] Thus ELF reflects the properties of the conditional pair density, that is, of the Lennard-Jones function. LJF requires the pair density for its evaluation, while ELF requires the one-electron density matrix; yet the information regarding the pairing of electrons yielded by both these functions is empirically determined by the topology of the Laplacian of the one-electron density.

One may begin to understand how information regarding the pair density is transmitted to the one-electron density in terms of the behavior of LJF. In the case of PH_3 for example, placing e* on a proton causes the Fermi hole to be strongly localized within the basin of the hydrogen atom, thereby leading to the formation of a nonbonding maximum in the same-spin density on the phosphorus atom with a percent exclusion in excess of 99%. Thus the conditional pair density in the nonbonded region reduces to the one-electron density, as shown in Figure 3f, and it is this density that yields the nonbonding charge concentration in the VSCC of the $L(\mathbf{r})$ distribution for the phosphorus atom.

References and Notes

(1) Lennard-Jones, J. *Adv. Sci., London* **1954**, *11*, 136.
(2) Lennard-Jones, J. *Proc. R. Soc. (London)* **1949**, *A198*, 14.
(3) Lennard-Jones, J.; Pople, J. A. *Proc.* R. *Soc. (London)* **1950**, *A202*, 166.
(4) Lennard-Jones, J. *J. Chem. Phys.* **1952**, *20*, 1024.
(5) Artmann, K. *Z. Naturwiss.* **1946**, *1*, 426.
(6) Zimmerman, H. K.; Van Rysselberghe, *J. Chem. Phys.* **1949**, *17*, 598.
(7) Linnett, J. W.; Poë, A. J. *Trans. Faraday. Soc.* **1951**, *47*, 1033.
(8) Gillespie, R. J.; Nyholm, R. S. *Q. Rev. Chem. Soc.* **1957**, *11*, 239; *Prog. Stereochem.* **1958**, *2*, 261.
(9) Gillespie, R. J.; Hargittai, I. *The VSEPR Model of Molecuar Geometry*; Prentice Hall: Englewood Cliffs, NJ, 1991.
(10) Gillespie, R. J.; Robinson, E. A. *Angew. Chem., Int. Ed. Engl.* **1996**, *35*, 495.
(11) McWeeny, R. *Rev. Mod. Phys.* **1960**, *32*, 335.
(12) Bader, R. F. W.; Stephens, M. E. *Chem. Phys. Lett.* **1974**, *26*, 445.
(13) Bader, R. F. W.; Stephens, M. E. *J. Am. Chem. Soc.* **1975**, *97*, 7391.
(14) Bader, R. F. W.; Johnson, S.; Tang, T.-H.; Popelier, P. L. A. *J. Phys. Chem.* **1996**, *100*, 15398.
(15) Bader, R. F. W.; MacDougall, P. J.; Lau, C. D. H. *J. Am. Chem. Soc.* **1984**, *106*, 1594. Bader, R. F. W.; Gillespie, R. J.; MacDougall, P. J. *J. Am. Chem. Soc.* **1988**, *110*, 7329.
(16) Becke, A. D.; Edgecombe, K. E. *J. Chem. Phys.* **1990**, *92*, 5397.
(17) The necessary and sufficient conditions imposed on a set of N spin-orbitals by the Pauli exclusion principle are that they be orthonormal and singly occupied. Thus approximate orbital theories that do not make explicit use of an antisymmetrized wave function in the minimization of the energy, but do meet the orthonormality requirement, as does the extended Hückel method for example, yield reasonable representations of the properties dependent upon the exclusion principle. This includes the electron localization function[16] that is based upon orbital representations of the kinetic energy.
(18) Bader, R. F. W. *Atoms in Molecules—A Quantum Theory*; Oxford University Press: Oxford, U.K., 1990.
(19) Bader, R. F. W. *Phys. Rev.* **1994**, *B49*, 13348.
(20) It is worth noting that the quantum mechanical equation of motion for the expectation value of an observable for an open system, that is, an atom in a molecule, requires that the atom be bounded in real space, a requirement that precludes the use of any orbital basis in the definition of atomic populations or other properties. An atomic population, for example, is the expectation value of the number operator averaged over the atomic basin.
(21) Frisch, M. J.; Trucks, G. W.; Schlegel, H. B.; Gill, P. M. W.; Johnson, B. G.; Robb, M. A.; Cheeseman, J. R.; Keith, T. A.; Petersson, J. A.; Montgomery, J. A.; Raghavachari, K.; Al-Laham, M. A.; Zakrzewski, V. G.; Ortiz, J. V.; Forseman, nJ. B.; Cioslowski, J.; Stefanov, B. B.; Nanayakkara, A.; Challacombe, M.; Peng, C. Y.; Ayala, P. Y.; Chen, W.; Wong, M. M.; Andres, J. L.; Replogle, E. S.; Gomperts, R.; Martin, R. L.; Fox, D. J.; Binkley, J. S.; Defrees, D. J.; Baker, J.; Stewart, J. P.; Head-Gordon, M.; Gonzalez, C.; Pople, J. A. *GAUSSIAN 94* (Revision B3); Gaussian, Inc.: Pittsburgh, PA, 1995.
(22) Silvi, B.; Savin, A. *Nature* **1994**, *371*, 683.
(23) Gillespie, R. J.; Bytheway, I.; Tang, T.-H.; Bader, R. F. W. *Inorg. Chem.* **1996**, *35*, 3954.
(24) Bader, R. F. W.; Gillespie, R. J.; Martín, F. *Chem. Phys. Lett.*, in press.
(25) Mayer, I. *Struct. Chem.* **1997**, *8*, 309.
(26) Tal, Y.; Bader, R. F. W. *Int. J. Quantum Chem., Quantum Chem. Symp.* **1978**, *12*, 153.